Applied Energy Symposium 2022: Clean Energy towards Carbon Neutrality (CEN2022)
April 23-25, 2022, Ningbo, China
Paper ID: 0115

Synthesis Strategies of Lead-free Double Perovskites Nanocrystals

Lingjun Wu[1], Wei Chen[1], Zijian Chen[1], Zixuan Wang[1], Hao Huang[1*], Haitao Zhao[1*], Xue-feng Yu[1]

1 Shenzhen Institute of Advanced Technology, Chinese Academy of Sciences, Shenzhen, Guangdong, China, 518055.
(*Corresponding Author)

ABSTRACT

Due to outstanding properties, the lead perovskites exhibit great potentials in optoelectronic applications, while still facing serious issues due to its high toxicity and instability. This necessitates the development of environmental-friendly lead-free double perovskites nanocrystals with low toxicity and tunable desired properties *via* size-control. In this review, we present the synthesis routines of lead-free perovskite nanocrystals, followed by detailed discussion of common characterization techniques and potential applications. This work is aimed for providing more insights in the property-tuning and synthesis of high-quality nano-size lead-free perovskites.

Keywords: lead-free metal halide double perovskite, nanocrystal, synthesis, photovoltaics

NONMENCLATURE

Abbreviations	
DP	Double perovskite
NC	Nanocrystal
PLQY	Photoluminescence quantum yield
XRD	X-ray Diffraction
SEM	scanning electron microscope
TEM	transmission electron microscope

1. INTRODUCTION

The lead halide perovskite $A^{I}Pb^{II}X_3$ ($A=CH_3NH_3$, Cs; X=Cl, Br, I) has aroused great attention due to its fabulous properties and wide usage in photovoltaic and optoelectronic applications. However, environmental issues triggered by the high toxicity of Pb remains an inevitable barrier to their commercial viability. It is therefore necessary to address this affair and develop alternative lead-free perovskite. In essence, categorization based on Pb-replacement strategies as well as the respective properties and drawbacks are presented in Figure 1(a), while more detailed design rules for lead-free perovskites are as illustrated in Figure 1 (b). At present, five main types of lead-free perovskites have rather to some extents, overcome or alleviated the two main issues of lead halide perovskites – the high toxicity and instability (Figure 1(a)). Among these newly developed types, the metal halide double perovskites (DP) with the formula $A_2B(I)B(III)X_6$, has aroused great attentions due to its excellent properties, and is considered a significant step towards ideal perovskites. Meanwhile the multiple tunable sites in the double perovskites endows it a rich chemistry.

However, one of the main challenges is the synthesis of DP nanocrystals (NC). It is well-recognized that the size has crucial impact on the material properties. For nano-size materials, the drastic change in properties compared to their macro analogues is indeed common. The significant increase of surface area in NC leads to high reactivities, and the quantum confinement effect also dramatically affects the material properties. In general, NCs exhibit better distribution in solvents, higher reactivities, and can act as perfect precursors for the fabrication of thin films. Thus, the size-control synthesis of DP NCs has become an extremely hot topic in the research community.

At present, some high-quality reviews on DPs have been reported [1],[2]. However, few of them have exclusively focused on the synthesis strategies of nano-size DPs. Moreover, with the increasing popularities, rapid achievement has been made in this field in recent

Selection and peer-review under the responsibility of the scientific committee of the CEN2022.

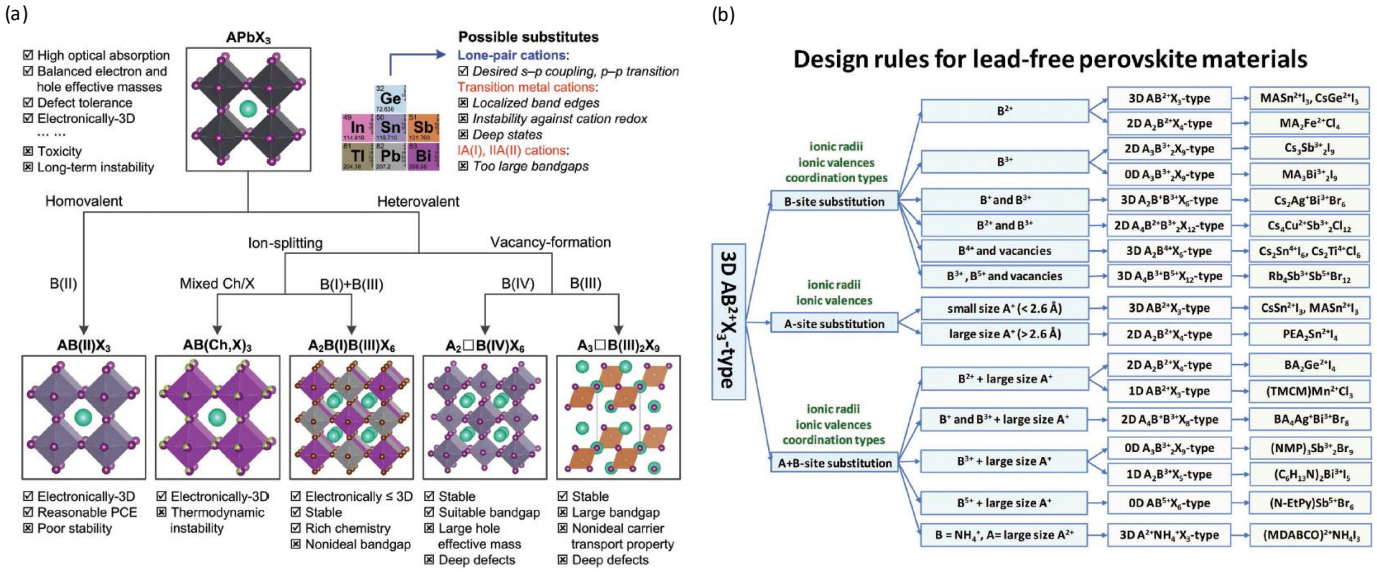

Fig. 1. a) Scheme of the approaches and results of potential lead replacement.[1] b) The design rules for lead-free perovskite materials.[2]

years. In this review, we focus on the synthesis strategies of DP NCs. Common characterization techniques and popular applications are also discussed as well, in a hope that our work can act as a guide and a source of inspiration for the development of novel lead-free perovskite materials.

2. THE SIZE EFFECT OF LEAD-FREE METAL HALIDE DOUBLE PEROVSKITES

The size of DP has a significant impact on its properties. Many studies have reported the huge differences of the optical properties of DP NCs compared to the bulk congeners [9]. As reported by Creutz *et al.*, the spectral features of the absorption spectra of $Cs_2AgBiBr_6$ and Cs_2AgBiI_6 of larger sizes are observed to red-shift [3]. This blue-shift of spectra peaks for NP NCs has been widely observed and attributed to the quantum confinement effect. Similar phenomenon has been observed for the ligand free $Cs_2AgBiBr_6$ NCs [4], the $Cs_2AgSbCl_6$ NCs [6], and the $Cs_2Ag_{1-x}Na_xInCl_6$ NCs [8].

However, there are different views on the quantum confinement effect. Han *et al.* surprisingly found that the PL emission of $Cs_2NaIn_{0.75}Bi_{0.25}Cl_6$:Mn NCs exhibits a red-shift compared to bulks. Meanwhile wider XRD peak was observed for NCs [9]. Dahl *et al.* pointed out that the discrepancies of DPs compared to their bulk congeners arise from differences in the measurement techniques

Table 1. Survey of morphology, size and synthetic method of double perovskites. Note: A:B refers to B as dopant in A.

Materials	size	Synthesis strategy	morphology	Ref.
$Cs_2AgInCl_6$/$Cs_2AgInCl_6$:Bi	9.79/10.95 nm	Hot-injection	crystal	[10]
$Cs_2AgBiBr_6$	3 mm	Hydrothermal method	crystal/ powder	[11]
Cs_2AgBiI_6	8-13 nm	Ion-exchange	crystal	[3]
$Cs_2AgInCl_6$/$Cs_2AgInCl_6$:Mn	9.8/11.6/12.6 nm	Hot-injection	crystal	[5]
Cs_2AgBX_6 (X=Br, Cl)	/	Precipitation/solid-state method	crystal	[12]
$Cs_2(Ag_{1-a}Bi_{1-b})TlxBr_6$/$(MA)_2TiBiBr_6$/$(MA)_2(Tl_{1-a}Bi_{1-6})AgxBr_6$	/	Hydrothermal method	Crystal/powder	[13]
$Cs_2AgIn_xBi_{1-x}Cl_6$	4.3 nm	Anti-solvent recrystallization	crystal	[14]
$Cs_2BiAgCl_6$	/	Solid-state method	Crystal/powder	[15]
$Cs_2NaIn_xBi_{1-x}Cl_6$/$Cs_2NaIn_xBi_{1-x}Cl_6$:Mn	10.93,10.59/9.43,10.45 nm	Hot-injection	crystal	[9]
$Cs_2InAgCl_6$	/	Precipitation method	powder	[16]
Cs_2AgBiX_6 (X=Cl, Br, I)	5 nm ($Cs_2AgBiBr_6$)	Anti-solvent recrystallization	crystal	[4]
Cs_2SnI_6	Several ten nm to several hundred nm	ultrasonic irradiation	crystal	[17]
$Cs_4CuSb_2Cl_{12}$	3 nm	ultrasonic exfoliation	crystal	[18]

and sample concentrations instead of the well-received quantum confinement [7]. It is concluded based on optical and theoretical analysis that both synthesized $Cs_2AgInCl_6$ and $Cs_2AgSbCl_6$ have nearly no quantum confinement. It is also observed by Dahl *et al.* that the orientation effects appear to affect the relative XRD peak intensities of $Cs_2AgInCl_6$ and $Cs_2AgSbCl_6$ NCs thin films in comparison to the bulk phase.

The size is also found to affect the emission lifetimes of NPs. As reported by Creutz *et al.*, long luminescence decay has been observed for both bulk and NC $Cs_2AgBiBr_6$, however for NCs, this is only observed at low temperatures. This is attributed to the suppression of surface trapping which contributes more for NCs [3]. It is found that the average PL lifetime of $Cs_2NaIn_{0.75}Bi_{0.25}Cl_6$:Mn NCs is longer than that of bulk crystals. The middle-lifetime process of bulk is not observed, which is attributed to the low surface defects trapping of bulks, especially doped ones [9].

DP NCs also show great color temperature (CT) tunability, while the CT of bulk congener is nearly fixed [8]. The temperature-dependent PL spectra for the optimized composition NCs of $Cs_2Ag_{0.17}Na_{0.83}In_{0.88}Bi_{0.12}Cl_6$ shows that the electron-phonon coupling strength decreases with reducing particle size under strong confinement, while the large Huang-Rhys factor of the $Cs_2Ag_{0.17}Na_{0.83}In_{0.88}Bi_{0.12}Cl_6$ NC suggests a relatively stronger electron-phonon coupling compared to traditional NCs, which favors the STE formation and high PLQY emission.

Apart from optical properties, the size effect also affects the stability. It is discovered that Cs_2AgBiI_6 could be stable in nanostructures, while may become unstable in bulk forms [4]. Meanwhile, it is found by Hu *et al*. that the $Cs_2Ag_{0.18}Na_{0.82}InCl_6$ NCs could be better characterized by TEM due to relatively better stability under electron beam irradiation [8]. Moreover, DP NCs are especially useful in the fabrication of thin films. The fabrications of high-quality crystalline thin films may be difficult if using bulk materials as the precursors due to poor solubility,[8] whereas the deposition of NCs is considered as a great alternative [5].

In conclusion, the size of DP is a significant factor in the determination of its properties, and NCs show various enhancement and superiority over the bulk congeners and deserves a more detailed investigation.

3. SYNTHESIS STRATEGIES OF LEAD-FREE DOUBLE PEROVSKITES NANOCRYSTALS

Table 1 summarizes the synthesis methods, their corresponding product morphologies, and sizes, which illustrate that NPs synthesized from different methods exhibit different sizes and morphologies. In this section, we will focus on the synthesis strategies of NP NCs.

3.1 Hot-injection

Typically, the hot-injection refers to the synthesis strategy where a precursor of the reaction is quickly injected to the mixture solution of remaining precursors under high temperature and inert atmosphere, as illustrated in Figure 2(b). The generated NCs are within a

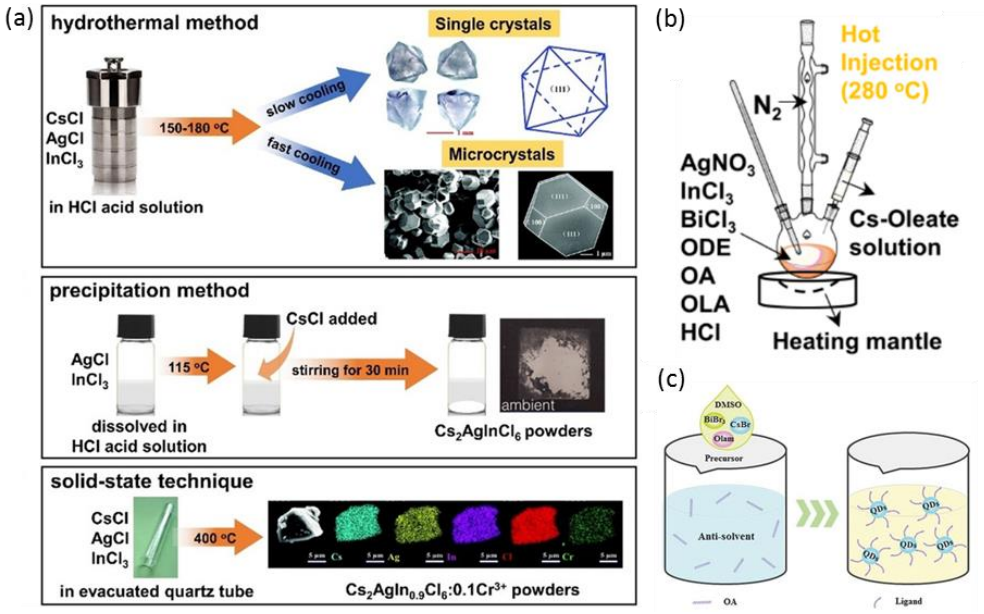

Fig. 2. Scheme of the synthesis strategies of perovskites of different sizes. a) synthesis method for bulk-size perovskites;[20] b) hot-injection approach;[10] c) anti-solvent method.[21]

narrow size distribution, accompanied with exhibition of prominent properties such as high crystallinity and great mono-dispersity [19].

Liu *et al.* synthesized undoped and Bi-doped $Cs_2AgInCl_6$ NCs using the hot-injection method [10]. PLQY as high as *ca.* 11.4% was observed. Locardi *et al.* proposed the first colloidal synthesis of size-controlled $Cs_2AgInCl_6$ NCs through hot-injection [5]. Han *et al.* used hot-injection approach for the synthesis of $Cs_2NaIn_xBi_{1-x}Cl_6$ and the Mn-doped counterpart [9].

3.2 Anti-solvent recrystallization

The anti-solvent recrystallization involves two main steps: first the precursors are dissolved in solvent A, which is then followed by the addition of solvent B with contrasting solubility, as illustrated in Figure 2(c). During the process, the wanted crystals are formed with ideal size and crystallinity. DP NCs with tunable bandgap was successfully synthesized by Yang *et al.* using the anti-solvent recrystallization approach [14].

3.3 Other approaches

Sidney *et al.* reported the success synthesis of unrecognized materials such as Cs_2AgBiI_6 through a post-synthetic modification of colloidal Cs_2AgBiX_6 (X = Cl, Br) NCs *via* anion exchange and cation extraction [3]. Koyanagi *et al.* synthesized Cs_2SnI_6 NCs using the ultrasonic irradiation method [17]. Mono-dispersed solution of produced particles has been prepared. Wang *et al* reported the synthesis of Single-layered $Cs_4CuSb_2Cl_{12}$ NCs *via* the ultrasonic exfoliation method [18].

Other synthesis strategies of DP also exist as summarized in Table 1, such as the hydrothermal method, the precipitation method, the solid-state method, *etc.* Nevertheless, these approaches are more commonly used for the synthesis of DP bulks, as shown in Figure 2(a), and are thereby not discussed herein.

It needs to be pointed out that most reported DP synthesis belongs to bulk or quantum dot level, while reports on medium-size DPs are still rare.

4. CHARACTERIZATION AND APPLICATIONS OF DOUBLE PEROVSKITES NANOCRYSTALS

4.1 Characterization techniques

Common characterization techniques for perovskite materials includes TEM, SEM, XRD, UV-Vis spectroscopy, etc., as demonstrated in Figure 3.

X-ray Diffraction (XRD). XRD works particularly well in the characterization of DPs' crystal structures, as shown in Figure 3 (a). XRD is useful for detecting the composition, structure, crystallinity, and crystal phase of the synthesized perovskites.

Optical spectroscopy. Common techniques including UV-Vis absorption/emission spectroscopy and photoluminescence spectroscopy are as shown in Figure 3(b). Optical spectroscopic features of DPs provide information of DPs' photo-properties, which is especially instructive for evaluating the DPs performance for potential related application.

Electron microscopy. The scanning electron microscope (SEM) and transmission electron microscope

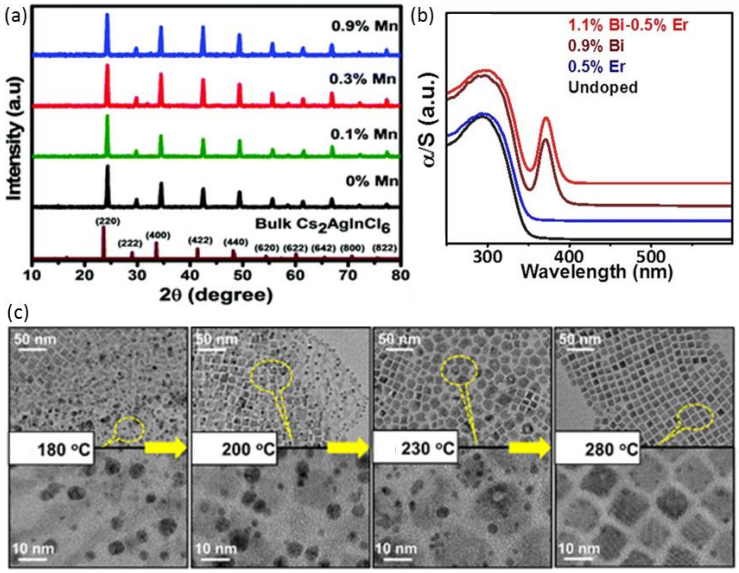

Fig. 3. Common characterization techniques used in DP synthesis. a) Powder XRD patterns for Mn-doped $Cs_2AgInCl_6$ with different Mn concentrations [22]; b) UV/Vis absorption spectra of Er^{3+} doped and Bi^{3+} -Er^{3+} codoped $Cs_2AgInCl_6$ [23]; c) TEM and HRTEM images of $Cs_2AgInCl_6$:Bi NCs under different synthesis temperatures [10].

(TEM) are most commonly used for obtaining high resolution images of DPs. Using electron microscopy, detailed information of structure and morphology can be obtained in a visual way, as shown in Figure 3(c). High-resolution TEM (HRTEM) can reach even higher resolution and is especially useful in nano-scale research.

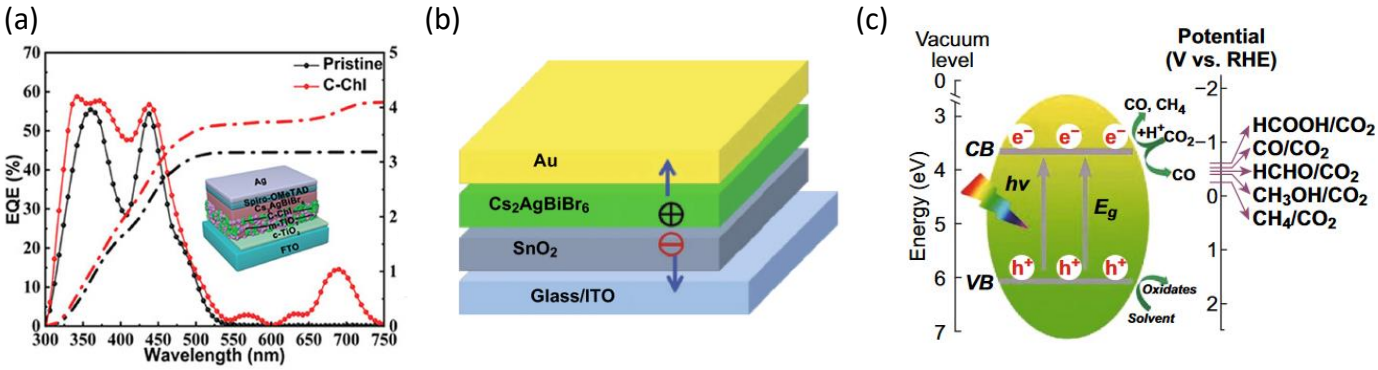

Fig. 4. Applications of DP NCs. a) the $Cs_2AgBiBr_6$ solar cells with inset illustrating the device structure [25]; b) the configuration of the $Cs_2AgBiBr_6$-based photodetector [24]; b) Scheme of the photoreduction of CO_2 on the surface of $Cs_2AgBiBr_6$ nanocrystals [24].

Other techniques. Other common characterization techniques include Raman spectroscopy, transient absorption spectroscopy, NMR, *etc.*

4.2 Applications

The absorptive and emissive nature of DPs upon irradiation endows it with the potential in various optoelectronic applications.

Solar cell. $Cs_2AgBiBr_6$ has been the most studied and applied DP-based solar cells. As aforementioned in Section 2, the solar cells require high-quality DP thin films, and deposition of NCs is considered a great strategy. Figure 4(a) illustrates the incorporation of carboxy-chlorophyll derivative on top of mesoporous TiO_2 which significantly boosted the performance of the $Cs_2AgBiBr_6$ solar cell.

Photocatalyst. $Cs_2AgBiBr_6$ NCs exhibits excellent stability against moisture, light, and temperature. It has thus been used as photocatalyst for CO_2 reduction with high selectivity, as illustrated in Figure 4(c). The tentative mechanism is the suitable conduction band of $Cs_2AgBiBr_6$ NCs which efficiently drives the reduction.

Photodetectors. The environmentally friendly DP-based photodetectors exhibit high stability and efficiency, and are excellent alternatives for lead-containing perovskite-based photodetectors. Figure 4(b) illustrates the high-performance self-powered $Cs_2AgBiBr_6$-based photodetector. The photogenerated carriers can be separated at the surface of the $Cs_2AgBiBr_6/SnO_2$ heterojunction by its built-in field.

Other applications. Other common applications include LEDs, X-ray detectors, ferroelectrics, *etc.*

Conclusion and Perspectives

The lead-free DP NC has great potential in photovoltaic applications in terms of its excellent properties. In this review, its synthesis strategy has been systematically reviewed, along with the brief summary of the characterization techniques and potential applications.

Despite considerable progress has been made so far in the synthesis of DP NCs, still several challenges exist in this field: First is an assured and decisive route to more precise size-control of DP NCs towards a narrower distribution range. Second is a more delicate morphology tuning of synthesized DP NCs that is desired for achieving ideal performance. Meanwhile, as most reported literatures are more inclined to the synthesis of quantum dot, the synthesis of DP NCs with medium size between quantum dot and bulk size is still rare.

Hopefully our work can provide a direction for future size-tuning and property enhancement for more novel perovskite materials.

ACKNOWLEDGEMENT

This work was supported by the National Natural Science Foundation of China (52173234), Shenzhen Science and Technology Program (JCY20210324102008023 and JSGG20210802153408024), Shenzhen-Hong Kong-Macau Technology Research Program (Type C, SGDX2020110309300301), Natural Science Foundation of Guangdong Province (2022A1515010554), and CCF-Tencent Open Fund. We thank Ningbo Municipal Key Laboratory on Clean Energy Conversion Technologies and the Zhejiang Provincial Key Laboratory for Carbonaceous Wastes Processing and Process Intensification Research funded by the Zhejiang Provincial Department of Science and Technology (2020E10018).

REFERENCE

[1] Xiao Z, Song Z, Yan Y. From Lead Halide Perovskites to Lead-Free Metal Halide Perovskites and Perovskite Derivatives. Advanced Materials 2019;31:1803792.

[2] Ning W, Gao F. Structural and Functional Diversity in Lead-Free Halide Perovskite Materials. Advanced Materials 2019;31:1900326.

[3] Creutz SE, Crites EN, De Siena MC, Gamelin DR. Colloidal Nanocrystals of Lead-Free Double-Perovskite (Elpasolite) Semiconductors: Synthesis and Anion Exchange To Access New Materials. Nano Lett 2018;18:1118–23.

[4] Yang B, Chen J, Yang S, Hong F, Sun L, Han P, et al. Lead-Free Silver-Bismuth Halide Double Perovskite Nanocrystals. Angewandte Chemie 2018;130:5457–61.

[5] Locardi F, Cirignano M, Baranov D, Dang Z, Prato M, Drago F, et al. Colloidal Synthesis of Double Perovskite $Cs_2AgInCl_6$ and Mn-Doped $Cs_2AgInCl_6$ Nanocrystals. J Am Chem Soc 2018;140:12989–95.

[6] Lv K, Qi S, Liu G, Lou Y, Chen J, Zhao Y. Lead-free silver-antimony halide double perovskite quantum dots with superior blue photoluminescence. Chemical Communications 2019;55:14741–4.

[7] Dahl JC, Osowiecki WT, Cai Y, Swabeck JK, Bekenstein Y, Asta M, et al. Probing the Stability and Band Gaps of $Cs_2AgInCl_6$ and $Cs_2AgSbCl_6$ Lead-Free Double Perovskite Nanocrystals. Chem Mater 2019;31:3134–43.

[8] Hu Q, Niu G, Zheng Z, Li S, Zhang Y, Song H, et al. Tunable Color Temperatures and Efficient White Emission from $Cs_2Ag_{1-x}Na_xIn_{1-y}Bi_yCl_6$ Double Perovskite Nanocrystals. Small 2019;15:1903496.

[9] Han P, Zhang X, Luo C, Zhou W, Yang S, Zhao J, et al. Manganese-Doped, Lead-Free Double Perovskite Nanocrystals for Bright Orange-Red Emission. ACS Cent Sci 2020;6:566–72.

[10] Liu Y, Jing Y, Zhao J, Liu Q, Xia Z. Design Optimization of Lead-Free Perovskite $Cs_2AgInCl_6$:Bi Nanocrystals with 11.4% Photoluminescence Quantum Yield. Chem Mater 2019;31:3333–9.

[11] Slavney AH, Hu T, Lindenberg AM, Karunadasa HI. A Bismuth-Halide Double Perovskite with Long Carrier Recombination Lifetime for Photovoltaic Applications. J Am Chem Soc 2016;138:2138–41.

[12] McClure ET, Ball MR, Windl W, Woodward PM. Cs_2AgBiX_6 (X = Br, Cl): New Visible Light Absorbing, Lead-Free Halide Perovskite Semiconductors. Chem Mater 2016;28:1348–54.

[13] Slavney AH, Leppert L, Bartesaghi D, Gold-Parker A, Toney MF, Savenije TJ, et al. Defect-Induced Band-Edge Reconstruction of a Bismuth-Halide Double Perovskite for Visible-Light Absorption. J Am Chem Soc 2017;139:5015–8.

[14] Yang B, Mao X, Hong F, Meng W, Tang Y, Xia X, et al. Lead-Free Direct Band Gap Double-Perovskite Nanocrystals with Bright Dual-Color Emission. J Am Chem Soc 2018;140:17001–6. https://doi.org/10.1021/jacs.8b07424.

[15] Volonakis G, Filip MR, Haghighirad AA, Sakai N, Wenger B, Snaith HJ, et al. Lead-Free Halide Double Perovskites via Heterovalent Substitution of Noble Metals. J Phys Chem Lett 2016;7:1254–9.

[16] Volonakis G, Haghighirad AA, Milot RL, Sio WH, Filip MR, Wenger B, et al. $Cs_2InAgCl_6$: A New Lead-Free Halide Double Perovskite with Direct Band Gap. J Phys Chem Lett 2017;8:772–8.

[17] Koyanagi T, Kapil G, Ogomi Y, Yoshino K, Shen Q, Toyoda T, et al. Hot-injection and ultrasonic irradiation syntheses of Cs_2SnI_6 quantum dot using Sn long-chain amino-complex. J Nanopart Res 2020;22:69.

[18] Wang X-D, Miao N-H, Liao J-F, Li W-Q, Xie Y, Chen J, et al. The top-down synthesis of single-layered $Cs_4CuSb_2Cl_{12}$ halide perovskite nanocrystals for photoelectrochemical application. Nanoscale 2019;11:5180–7.

[19] Tang H, Xu Y, Hu X, Hu Q, Chen T, Jiang W, et al. Lead-Free Halide Double Perovskite Nanocrystals for Light-Emitting Applications: Strategies for Boosting Efficiency and Stability. Advanced Science 2021;8:2004118.

[20] Liu Y, Nag A, Manna L, Xia Z. Lead-Free Double Perovskite $Cs_2AgInCl_6$. Angewandte Chemie 2021;133:11696–707.

[21] Leng M, Yang Y, Zeng K, Chen Z, Tan Z, Li S, et al. All-Inorganic Bismuth-Based Perovskite Quantum Dots with Bright Blue Photoluminescence and Excellent Stability. Advanced Functional Materials 2018;28:1704446.

[22] Nandha K N, Nag A. Synthesis and luminescence of Mn-doped $Cs_2AgInCl_6$ double perovskites. Chemical Communications 2018;54:5205–8.

[23] Arfin H, Kaur J, Sheikh T, Chakraborty S, Nag A. Bi3+-Er^{3+} and Bi^{3+}-Yb^{3+} Codoped $Cs_2AgInCl_6$ Double Perovskite Near-Infrared Emitters. Angewandte Chemie International Edition 2020;59:11307–11.

[24] Chu L, Ahmad W, Liu W, Yang J, Zhang R, Sun Y, et al. Lead-Free Halide Double Perovskite Materials: A New Superstar Toward Green and Stable Optoelectronic Applications. Nano-Micro Lett 2019;11:16.

[25] Lei H, Hardy D, Gao F. Lead-Free Double Perovskite $Cs_2AgBiBr_6$: Fundamentals, Applications, and Perspectives. Advanced Functional Materials 2021;31:2105898.